OCEANOLOGICA ACTA · VOL. 23 - N° 1

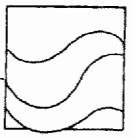

# Vertical structure of the semidiurnal tidal currents at Camarinal Sill, the strait of Gibraltar

**Miguel BRUNO [a]*, Rafael MAÑANES [a], José Juan ALONSO [a], Alfredo IZQUIERDO [a], Luis TEJEDOR [a], Boris A. KAGAN [b]**

[a] Departamento de Física Aplicada, Universidad de Cádiz, Polígono del Río San Pedro s/n 11510, Puerto Real, Cadiz, Spain
[b] P.P Shirshov Institute of Oceanology, Russian Academy of Sciences, St. Petersburg Branch, Russia

Received 23 July 1998; revised 6 May 1999; accepted 25 May 1999

**Abstract** – The dynamical mode decomposition (DMD) technique is applied to the data of currentmeter and CTD measurements taken during the 1985–1986 Gibraltar Experiment and the 1989 survey so as to clarify features of the vertical structure of the $M_2$ and $S_2$ tidal currents at the Camarinal Sill. It is shown that in conformity with the inference made on the basis of the empirical orthogonal function (EOF) decomposition technique, these currents are mainly due to the $M_2$ and $S_2$ barotropic modes. At the same time the first three baroclinic modes are responsible not only for the vertical variability of the tidal currents but also for the velocity and density amplitude variances at semidiurnal frequencies. Certain quantitative discrepancies between the values of barotropic tidal current characteristics as deduced from DMD and EOF decomposition techniques are revealed. In order to eliminate these, new currentmeter data are required with a finer vertical resolution than those which are available. © 2000 Ifremer/CNRS/IRD/Éditions scientifiques et médicales Elsevier SAS

**barotropic and baroclinic modes / tidal current / dynamical mode decomposition / Strait of Gibraltar**

**Résumé – Structure verticale des courants de marée semi-diurne sur le seuil du détroit de Gibraltar.** La structure verticale des courants de marée $M_2$ et $S_2$ sur le seuil Camarinal a été étudiée en appliquant la technique de décomposition en mode dynamique (DMD) aux données de courantométrie et d'hydrologie de l'expérience Gibraltar 1985-1986 et à celles de la campagne 1989. Les résultats, en accord avec l'analyse par fonctions empiriques orthogonales (EOF), indiquent que les courants sont engendrés par les modes barotropes $M_2$ et $S_2$. Les trois premiers modes baroclines sont responsables de la variabilité verticale des courants de marée et des variances d'amplitude de la vitesse et de la densité aux fréquences semi-diurnes. Certains écarts quantitatifs apparaissent entre les valeurs des caractéristiques du courant de marée barotrope obtenues par les techniques de décomposition DMD et EOF. Pour éliminer ces écarts, il faudrait disposer de nouvelles données de courantométrie avec une meilleure résolution verticale. © 2000 Ifremer/CNRS/IRD/Éditions scientifiques et médicales Elsevier SAS

**modes barotrope et barocline / courant de marée / décomposition en mode dynamique / détroit de Gibraltar**

## 1. INTRODUCTION

Tidal velocities are usually separated into barotropic and baroclinic components by employing either an empirical orthogonal function (EOF) decomposition

* Correspondence and reprints: miguel.bruno@uca.es


PII: S0399-1784(00)00104-3/FLA

[2–4] or a dynamical mode decomposition (DMD) [3, 5–8]. With the DMD, a set of the vertical dynamical modes of the pressure (or another flow characteristic) field at a given mean vertical distribution of the sea-water density is obtained from a solution of the hydrodynamics equations for incompressible, inviscid fluid under some assumptions of flow dynamics and bottom topography. A least-square estimation procedure is then used to determine the modal amplitudes and phases from the observed values of tidal velocity at different depths.

The EOF decomposition does not need these assumptions, so that the resulting EOFs are solely determined by the statistics of the data in use. The EOFs, however, are difficult to interpret in terms of their physical origin. In fact, a standard practice is to consider the first EOF as a barotropic (depth-independent) mode, although on closer examination the rms velocity values (weights) due to this EOF, say, at the Camarinal Sill cross-section, are noted to decrease by half with depth [2]. Moreover, the EOF decomposition is limited to a weight time series analysis and may thus distort real spatial phase distributions [1]. In addition, the EOF decomposition allows barotropic and baroclinic components of tidal velocity to be separated only if they are orthogonal; otherwise, their separation with different temporal weights is impossible even when current-meter data with a fine vertical resolution are available. Clearly, neither decomposition technique is without disadvantages.

In such a situation, the only solution is to employ both of these techniques so as to demonstrate that they produce consistent results. It is that approach which has been applied to the analysis of the current velocity time series on the continental shelf off the Oregon coast [3] and in the Canary and Iberian basins of the North Atlantic [6]. These techniques, as applied to the Strait of Gibraltar, have never been utilized together, and the only information we have had to date contains the estimates of the barotropic and baroclinic tidal velocity components obtained exclusively on the basis of the EOF decomposition technique [2, 4]. In accordance with these estimates, the semidiurnal velocity variance at the Camarinal Sill is mainly due to the barotropic mode, while under 10 % of the variance falls on the baroclinic modes.

This fact, as well as noticeable discrepancies between the EOF decomposition estimates of the semidiurnal barotropic tidal velocity and the predictions provided by a 2D high-resolution, nonlinear, boundary-fitted co-ordinate tidal model for the Strait of Gibraltar [9], make it necessary to seek a further independent verification of the above inference. The DMD technique may be invoked for this purpose. The aim of the present paper is twofold: i) to provide, by employing the DMD, new estimates of the barotropic and baroclinic tidal current characteristics and their associated velocity and density amplitude variances for the $M_2$ and $S_2$ constituents at the Camarinal Sill; and ii) to compare these estimates with those deduced from the EOF decomposition so as to determine the extent to which both of these estimates are in line with each other.

The paper is organized as follows: in Section 2 the theoretical description of the DMD technique is briefly reviewed. Section 3 describes the data used. In Section 4 the results are discussed. Conclusions involve a comparison of the barotropic and baroclinic tidal velocity characteristics at the Camarinal Sill as deduced from the DMD and EOF decomposition techniques.

## 2. DYNAMICAL MODE DECOMPOSITION

The DMD starts from hydrodynamics equations with the assumptions that the fluid is horizontally unbounded, linear and Boussinesq and that dissipative effects as well as the effects associated with the horizontal inhomogeneity of ambient stratification are negligible. In this case, the initial set of equation of motion, conservation of density and continuity reads

$$\frac{\partial u}{\partial t} - fv = -\frac{1}{\rho_0}\frac{\partial p}{\partial x} \tag{1}$$

$$\frac{\partial v}{\partial t} + fu = -\frac{1}{\rho_0}\frac{\partial p}{\partial y} \tag{2}$$

$$\frac{\partial w}{\partial t} = -\frac{1}{\rho_0}\frac{\partial p}{\partial z} - \frac{g}{\rho_0}\rho \tag{3}$$

$$\frac{\partial \rho}{\partial t} - \frac{N^2\rho_0}{g}w = 0 \tag{4}$$

$$\frac{\partial u}{\partial x} + \frac{\partial v}{\partial y} + \frac{\partial w}{\partial z} = 0 \tag{5}$$

where $u$ and $v$ are the eastward and northward components of the velocity vector in the Cartesian co-

ordinate system $(x, y, z)$; $w$ is the vertical component of velocity; $p$ and $\rho$ are the perturbations of pressure and density; $\rho_0$ is the mean sea-water density; $N$ is the buoyancy frequency defined as

$$N(z) = \sqrt{-(g/\rho_0)(\mathrm{d}\rho_0/\mathrm{d}z)}$$

$g$ is the acceleration due to gravity; $f$ is the Coriolis parameter; and $z$ is the vertical co-ordinate directed upward.

With the rigid-lid approximation eliminating the barotropic mode from consideration and the flat-bottom assumption justified for baroclinic modes with wavelengths much smaller than characteristic topographic lengthscales, the boundary conditions at the surface $(z = D)$ and the bottom $(z = 0)$ are

$$P = 0, w = 0 \quad \text{for} \quad z = D \tag{6}$$

$$w = 0 \quad \text{for} \quad z = 0 \tag{7}$$

For a harmonic oscillation with a given tidal frequency $\omega$, the complex amplitudes of the variables sought may be presented as

$$\tilde{u}(x, y, z) = \frac{1}{\rho_0} \sum_{n=1}^{\infty} P_n(z) U_n(x, y) \tag{8}$$

$$\tilde{v}(x, y, z) = \frac{1}{\rho_0} \sum_{n=1}^{\infty} P_n(z) V_n(x, y) \tag{9}$$

$$\tilde{w}(x, y, z) = i\omega \sum_{n=1}^{\infty} W_n(z) \Pi_n(x, y) \tag{10}$$

$$\tilde{p}(x, y, z) = \sum_{n=1}^{\infty} P_n(z) \Pi_n(x, y) \tag{11}$$

$$\tilde{\rho}(x, y, z) = \sum_{n=1}^{\infty} \frac{\mathrm{d}P_n(z)}{\mathrm{d}z} \Gamma_n(x, y) \tag{12}$$

On substituting eqs. (8) to (12) into eqs. (1) to (5) and introducing the separation constant $|k_n|$ (here $k_n$ is the mode $n$ wavenumber), we obtain the equation

$$\frac{\mathrm{d}}{\mathrm{d}z}\left[\frac{(\omega^2 - f^2)}{(N^2 - \omega^2)} \frac{\mathrm{d}P_n}{\mathrm{d}z}\right] + \frac{N^2}{g} \frac{(\omega^2 - f^2)}{(N^2 - \omega^2)} \frac{\mathrm{d}P_n}{\mathrm{d}z} + |k_n|^2 P_n = 0 \tag{13}$$

which describes the variation of the pressure amplitude along the vertical. If one normalizes the tidal frequency $\omega$ and the buoyancy frequency $N$ by $f$, and the height $z$ by $D$, then on retaining the same designations eq. (13) is rewritten as

$$\frac{\mathrm{d}}{\mathrm{d}z}\left[\frac{(\omega^2 - 1)}{(N^2 - \omega^2)} \frac{\mathrm{d}P_n}{\mathrm{d}z}\right] + \mu N^2 \frac{(\omega^2 - 1)}{(N^2 - \omega^2)} \frac{\mathrm{d}P_n}{\mathrm{d}z} + |k_n|^2 P_n = 0 \tag{14}$$

where $\mu = D(f^2/g)$ is a dimensionless parameter.

In terms of $P_n$ the boundary conditions (6) and (7) become

$$P_n = 0 \text{ at } z = 1 \tag{15}$$

$$\frac{\mathrm{d}P_n}{\mathrm{d}z} = 0 \text{ at } z = 0 \tag{16}$$

Thus, if the dimensionless buoyancy frequency profile $N(z)$ and the dimensionless frequency $\omega$ are prescribed, the problem considered is reduced to the eigenvalue problem (14) to (16), the solution of which is a linear superposition of a set of eigenfunctions $P_n(z)$, vertical dynamical modes, satisfying the orthogonality condition

$$\int_0^1 P_n(z) P_m(z)\, \mathrm{d}z = \delta_{nm} \tag{17}$$

with eigenvalues $|k_n|^2$. Here $\delta_{nm}$ is the Kronecker delta.

Note that when condition (17) is replaced by its discrete analogue, the orthogonality properties of the eigenfunctions $P_n(z)$ can be impaired, so that Eq. (17) cannot serve to determine the modal amplitudes. For this purpose a least-square estimation procedure is commonly used, which fits the vertical dynamical modes to observational data. Accordingly, the observed complex amplitudes of tidal velocity and density at a given location with the co-ordinates $(x, y, z_j)$, $z_j$ being specified by the sampling heights, are represented as series of modal amplitudes $U_n$, $V_n$ and $\Gamma_n$ by

$$\tilde{u}(x, y, z_j) = \tilde{u}_0 + \sum_{n=1}^{M} P_n(z_j) U_n(x, y) \tag{18}$$

$$\tilde{v}(x, y, z_j) = \tilde{v}_0 + \sum_{n=1}^{M} P_n(z_j) V_n(x, y) \tag{19}$$

$$\tilde{\rho}(x, y, z_j) = \sum_{n=1}^{M} \left.\frac{\mathrm{d}P_n(z)}{\mathrm{d}z}\right|_{z_j} \Gamma_n(x, y) \tag{20}$$

where $M$ is the number of baroclinic modes being held in fitting; the subscript '0' denotes the barotropic components of tidal velocity.

## 3. THE DATA SET

The data in use include observational data of two kinds: CTD temperature and salinity time series on the one hand, and current velocity, temperature and salinity time series taken from currentmeter measure

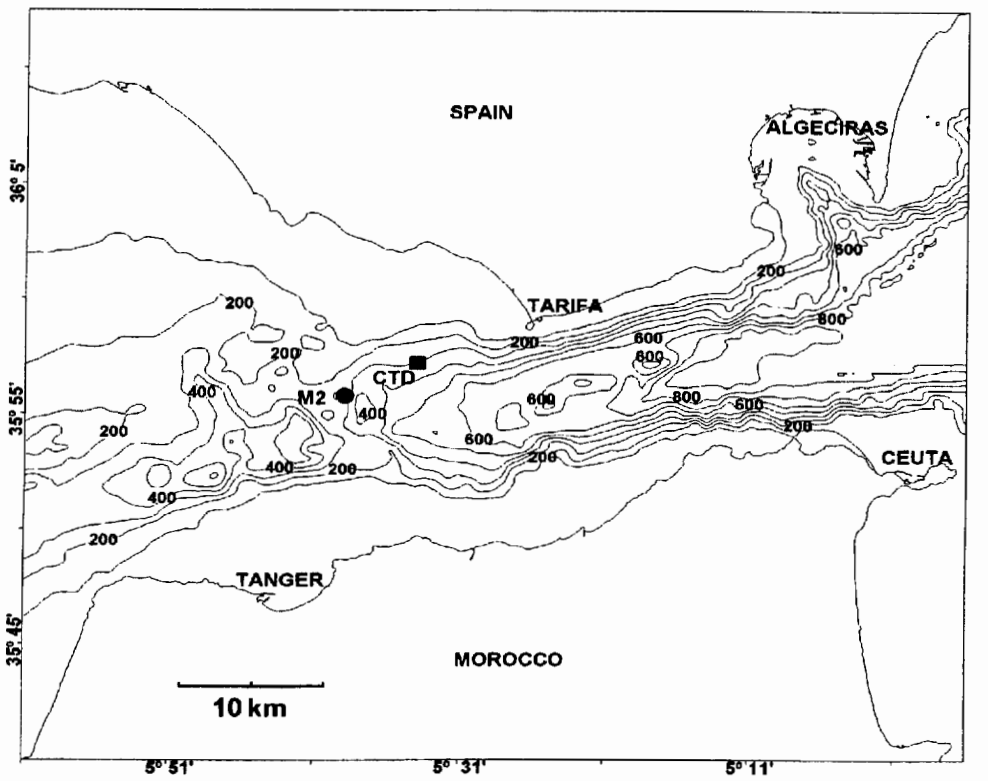


**Figure 1.** Map of the Strait of Gibraltar with the bottom topography (isobaths in meters) and the locations of the mooring M2 and the CTD station.

ments on the other hand. The CTD data were obtained during the survey performed by the Army Hydrographic Institute of Cádiz (Spain) in October 1989. These were sampled at the location shown in *figure 1* at a rate of one hour every 24 h. The data on pressure, temperature and salinity had 2-m-vertical resolution, from the depth of 1 m. As the CTD dropped with a velocity of 1 $m \cdot s^{-1}$ throughout a vertical distance of over 200 m, the time spent for performing each set of measurements was less than 4 min, and so all the records corresponding to the same set may be regarded as being simultaneous.

The current velocity, temperature and salinity time series were provided by the mooring M2 deployed during the 1985–1986 Gibraltar Experiment. This mooring located roughly midway along the Camarinal Sill cross-section (*figure 1*) was chosen because it had a better vertical resolution within the upper layer than the moorings M1 and M3. The mooring M2 was deployed for the two measuring periods: from 22 October 1985 to 4 May 1986 and from 29 May 1986 to 13 October 1986. During the first of these periods the upper layer above the interface between the Atlantic and Mediterranean waters (its mean depth is about 130 m [1]) was less well resolved than during the second period: the moored currentmeters were deployed at a depth of 123 m for the first period and the depths of 90 and 120 m for the second one. It is therefore the second measuring period that was chosen for analysis.

As known, the predominant tidal signals in the Strait of Gibraltar have the $M_2$ and $S_2$ frequencies. So we now need to focus upon these signals.

## 4. RESULTS AND DISCUSSION

The vertical profile of the dimensionless buoyancy frequency $N$ obtained by time averaging the CTD data

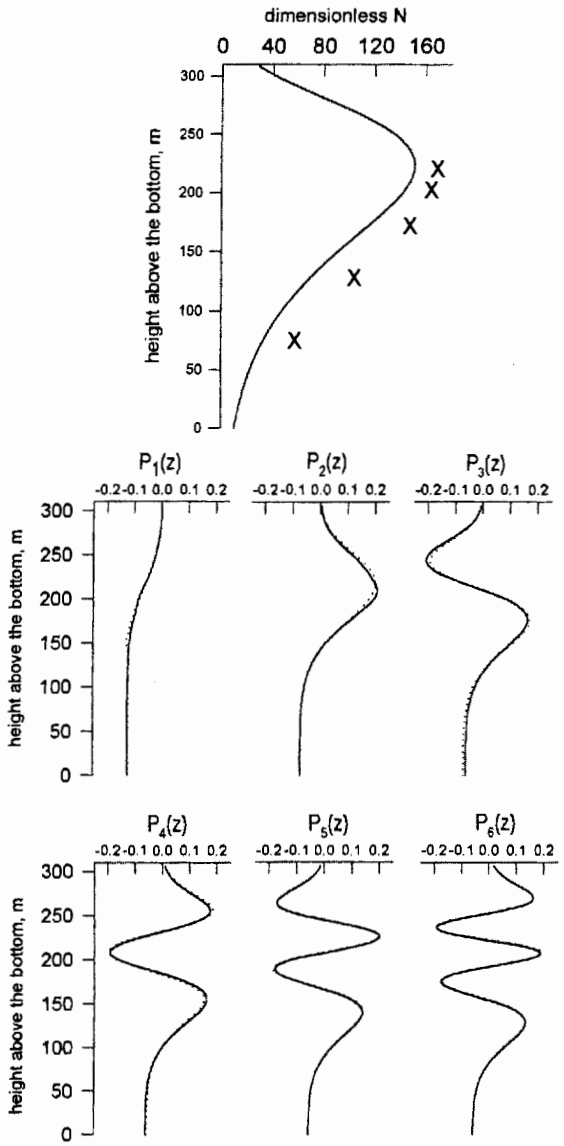


**Figure 2.** Vertical profile of the dimensionless buoyancy frequency $N$ and the first six vertical dynamical modes $P_n$ ($n = 1, \ldots, 6$) with the $M_2$ (solid lines) and $S_2$ (dotted lines) frequencies. Also shown are the $N$-values (crosses) obtained by the temperature and salinity data at the mooring $M_2$.

at 70 measurement depths from 1 m to 155 m is shown in *figure 2*. Here also shown are the $N$-values derived from temperature and salinity measurements at the mooring $M_2$. They are evidently close to the above vertical profile. In addition, *figure 2* displays the first six vertical dynamical modes $P_n(z)$, n = 1, ..., 6, whose distinctions for the dimensionless $M_2$ and $S_2$ frequencies are hardly visible. The modes are numbered in order of increasing eigenvalue $|k_n|^2$.

Before proceeding to the results of the least-square fitting of the observed tidal velocity amplitudes with the vertical dynamical modes, some additional remarks need to be made. First, no account has to be taken in the fitting for evidence from currentmeter measurement in the near-bottom layer as being inevitably affected by bottom friction effects. If so, we have currentmeter data only at five depths. With such a body of data, care must be exercised in choosing the number of the vertical dynamical modes and, in any case, a reasonable number of degrees of freedom (NDF) should be evaluated. The recommended minimum value for the NDF is usually 11 [7, 8]. On defining the NDF as NDF $= 4N-3M$ (here $N$ is the number of the sampling depths, and $M$ is the number of the vertical dynamical modes to be included in fitting), we obtain $M = 3$ at NDF = 11. That is, with this value of the NDF the set of the vertical dynamical modes has to comprise only the barotropic mode and any two baroclinic modes.

Second [2, 4], the tidal velocity variability at the Camarinal Sill is mainly controlled by the barotropic modes with semidiurnal frequencies. It follows that the contribution of all the baroclinic modes with the same frequencies to the tidal velocity variability represents a small difference of two large quantities and, hence, the evaluation of baroclinic modal amplitudes by the least-square fitting will entail great errors. To eliminate these errors it makes sense to exclude the barotropic modes. This can be arranged by transforming the sets (18) and (19) into new sets of the differences $\Delta\tilde{u}(z_j)$, $\Delta\tilde{v}(z_j)$ between the observed tidal velocity amplitudes $\tilde{u}(z_j)$, $\tilde{v}(z_j)$ at the sampling heights $z_j$ and their values at a fixed height $z_l$ so as then to fit these differences

$$\Delta\tilde{u}(z_j) = \sum_{n=1}^{M} U_n[P_n(z_j) - P_n(z_l)] \tag{21}$$

$$\Delta\tilde{v}(z_j) = \sum_{n=1}^{M} V_n[P_n(z_j) - P_n(z_l)] \tag{22}$$

with the transformed vertical dynamical modes $[P_n(z_j) - P_n(z_l)]$.

Finally, as *figure 2* shows, the first vertical dynamical mode cannot be precisely fitted because its discrete

analogue is similar to a linear combination of the discretely sampled second and third modes. This difficulty may be resolved by either excluding the first baroclinic mode from consideration or setting limits on the value of the baroclinic component of tidal velocity. Otherwise, as has been established in a preliminary test, the least-square fitting provides the unrealistic values of the baroclinic components of the $M_2$ and $S_2$ tidal velocity amplitudes that may be as much as 4 $m \cdot s^{-1}$. We preferred to use the second way as a less restrictive one assuming, on a priori grounds, that the $M_2$ and $S_2$ baroclinic tidal velocity amplitudes cannot exceed the barotropic ones.

With allowance made for the above, the first three vertical dynamical modes were applied to the fitting of eqs. (21) and (22). Thereafter, the derived values of $U_n$ and $V_n$ were used to reconstruct the vertical structure of the $M_2$ and $S_2$ baroclinic tidal currents. Given the baroclinic components, the barotropic ones were determined by substracting the former from the observed values of $\tilde{u}(z_j)$ and $\tilde{v}(z_j)$ followed by averaging the residuals over height. The resulting barotropic and baroclinic components of the $M_2$ and $S_2$ tidal velocities are presented, in terms of tidal current ellipse parameters, in *table I*.

Even a cursory inspection of this table reveals some specific features of the vertical structure of the $M_2$ and $S_2$ tidal currents at the Camarinal Sill; namely, i) these currents are mainly due to the $M_2$ and $S_2$ barotropic modes, as has been reported by Candela et al. [2] and Mañanes et al. [4]; ii) the first baroclinic modes are of secondary importance to the second and third baroclinic modes with the $M_2$ and $S_2$ frequencies; iii) the influence of the second and third baroclinic modes is most conspicuous at the heights where these have maxima, that is, at the heights of 220 and 198 m for the $M_2$ and $S_2$ second modes and at the heights of 198 and 175 m for the $M_2$ and $S_2$ third modes; and iv) the $M_2$ and $S_2$ second-mode signals at the heights of 220, 198 and 175 m and the $M_2$ and $S_2$ third-mode signals at the heights of 220, 198, 175 and 129 m are out of phase with those at lower heights. As is evident from *figure 2*, this is because the second modes have zero crossings at about 156 m, while the third modes have zero crossings at about 126 and 232 m.

The inferences about a crucial effect of the barotropic modes and a profound impact of the second and third baroclinic modes on the formation of the $M_2$ and $S_2$ tidal currents at the Camarinal Sill are confirmed by comparing the relative velocity variances presented in *table II*. Here the normalizing factor used in evaluating the relative velocity variance at each height is set equal to the variance corresponding to the superposition of the modes considered.

*Figure 3* demonstrates a comparison of the predicted tidal current ellipse parameters with their observed values at different heights. Notice that these parameters were obtained by the superposition of the barotropic mode and the first three baroclinic modes only. In this connection the question arises as to whether this set of modes is sufficient to describe the vertical structure of another tidal characteristic which is known in detail (say, tidal density perturbation). In order to answer this question the relative semidiurnal density amplitude variances at different heights were determined by fitting the observed values of $\overline{\rho}$ to the vertical dynamical modes as required by eq. (20). The semidiurnal signal was chosen for analysis since the available density time series (their duration was 1 day only) prevent the $M_2$ and $S_2$ signals from being separated. Unlike the tidal velocity amplitude and phase, the tidal constants for density perturbations were obtained by filtering the initial density time series, so that the semidiurnal signal will be extracted, followed by a least-square harmonic analysis. In evaluating the relative density amplitude variances for individual modes the normalizing factor was taken equal to the observed values of the variance at different heights.

The calculation results are given in *figure 4*. As is easy to see, the relative density amplitude variance increases with decreasing mode wavenumber. In other words, the vertical structure of the semidiurnal density variability is mainly due to the lower-order modes and may be evaluated with reasonable accuracy only by the first three vertical dynamical modes. Also it is clear that the first baroclinic mode accounts for the majority of the semidiurnal density variance at the heights of about 250 m. This is inconsistent with the DMD results for the semidiurnal velocity variance.

The question now is: why do the contributions of the first baroclinic mode to the observed velocity and density variances diverge considerably? One should expect that the probable chief cause is the improper vertical distribution of currentmeters which renders quantification of the first baroclinic mode impossible.

To verify that this is indeed so, we repeated the modal decomposition of the semidiurnal density signal using, as the basis, the density time series only at those five (or nearly) heights at which the DMD technique has been applied to the currentmeter data. The results of this experiment on the sensitivity of the DMD to the vertical distribution of measurements are shown in *figure 5*. A comparison of *figures 4* and

**Table I.** Tidal current ellipse parameters for the barotropic and baroclinic modes and their superposition at the $M_2$ and $S_2$ frequencies[a]

| Mode | Height | $M_2$ wave | | | | $S_2$ wave | | | |
|---|---|---|---|---|---|---|---|---|---|
| | | M ($cm \cdot s^{-1}$) | (m) ($cms^{-1}$) | θ (deg) | g (deg) | M ($cm \cdot s^{-1}$) | (m) ($cms^{-1}$) | θ (deg) | g (deg) |
| 0 | — | 85.18 | −0.60 | 21.75 | 143.72 | 31.47 | −1.12 | 19.99 | 172.53 |
| 1 | 220 | 5.74 | −3.92 | 343.05 | 125.65 | 2.59 | −1.04 | 5.63 | 140.93 |
| | 198 | 7.01 | −4.82 | | | 3.16 | −1.27 | | |
| | 175 | 8.09 | −5.57 | | | 3.65 | −1.46 | | |
| | 129 | 9.37 | −6.44 | | | 4.23 | −1.70 | | |
| | 77 | 9.60 | −6.60 | | | 4.33 | −1.74 | | |
| 2 | 220 | 35.90 | 0.98 | 331.31 | 124.72 | 14.49 | −1.12 | 307.27 | 149.63 |
| | 198 | 26.91 | 0.73 | | 124.72 | 8.62 | −0.84 | | 149.63 |
| | 175 | 14.39 | 0.39 | | 124.72 | 4.60 | −0.45 | | 149.63 |
| | 129 | 7.05 | 0.19 | | 304.72 | 2.56 | −0.22 | | 329.63 |
| | 77 | 15.08 | 0.41 | | 304.72 | 4.83 | −0.47 | | 329.63 |
| 3 | 220 | 7.90 | −1.87 | 5.09 | 207.33 | 3.59 | 0.18 | 28.21 | 218.00 |
| | 198 | 26.29 | −6.24 | | 207.33 | 11.96 | 0.62 | | 218.00 |
| | 175 | 29.83 | −7.09 | | 207.33 | 13.57 | 0.70 | | 218.00 |
| | 129 | 6.77 | −1.61 | | 207.33 | 3.08 | 0.16 | | 218.00 |
| | 77 | 9.57 | −2.27 | | 27.33 | 4.35 | 0.22 | | 38.00 |
| Modal superposition | 220 | 118.10 | 3.13 | 7.12 | 141.28 | 40.27 | 1.10 | 4.17 | 169.95 |
| | 198 | 121.29 | −2.67 | 10.75 | 149.76 | 45.26 | −0.61 | 10.10 | 178.33 |
| | 175 | 115.47 | −7.74 | 13.91 | 152.58 | 45.55 | −2.62 | 14.29 | 180.46 |
| | 129 | 89.71 | −7.81 | 20.75 | 144.25 | 36.38 | −3.40 | 20.93 | 172.46 |
| | 77 | 77.93 | −3.70 | 24.30 | 135.12 | 31.04 | −2.36 | 24.23 | 163.81 |

[a] M is the semi-major axis; m is the semi-minor axis; θ is the orientation of the semi-major axis; g is the Greenwich phase (time of occurrence of the maximum tidal current with respect to the GMT). The sign of the semi-minor axis indicates the sense of rotation of the tidal current (positive counterclockwise); orientation corresponds to maximum flood current into the Mediterranean and is measured from the east.

**Table II.** Relative velocity variance (in percentage) for the barotropic and baroclinic modes with the $M_2$ and $S_2$ frequencies

| Height (m) | $M_2$ mode | | | | $S_2$ mode | | | |
|---|---|---|---|---|---|---|---|---|
| | 0 | 1 | 2 | 3 | 0 | 1 | 2 | 3 |
| 220 | 83.86 | 0.38 | 15.03 | 0.73 | 86.72 | 0.54 | 11.57 | 1.13 |
| 198 | 83.07 | 0.57 | 8.37 | 7.99 | 81.33 | 0.82 | 6.10 | 11.75 |
| 175 | 86.05 | 0.78 | 2.48 | 10.66 | 81.91 | 1.10 | 1.76 | 15.23 |
| 129 | 97.51 | 1.19 | 0.67 | 0.62 | 96.83 | 1.75 | 0.50 | 0.93 |
| 77 | 94.59 | 1.21 | 2.99 | 1.21 | 94.19 | 1.79 | 2.20 | 1.80 |
| Mean | 89.01 | 0.82 | 5.91 | 4.24 | 88.19 | 1.21 | 4.43 | 6.18 |

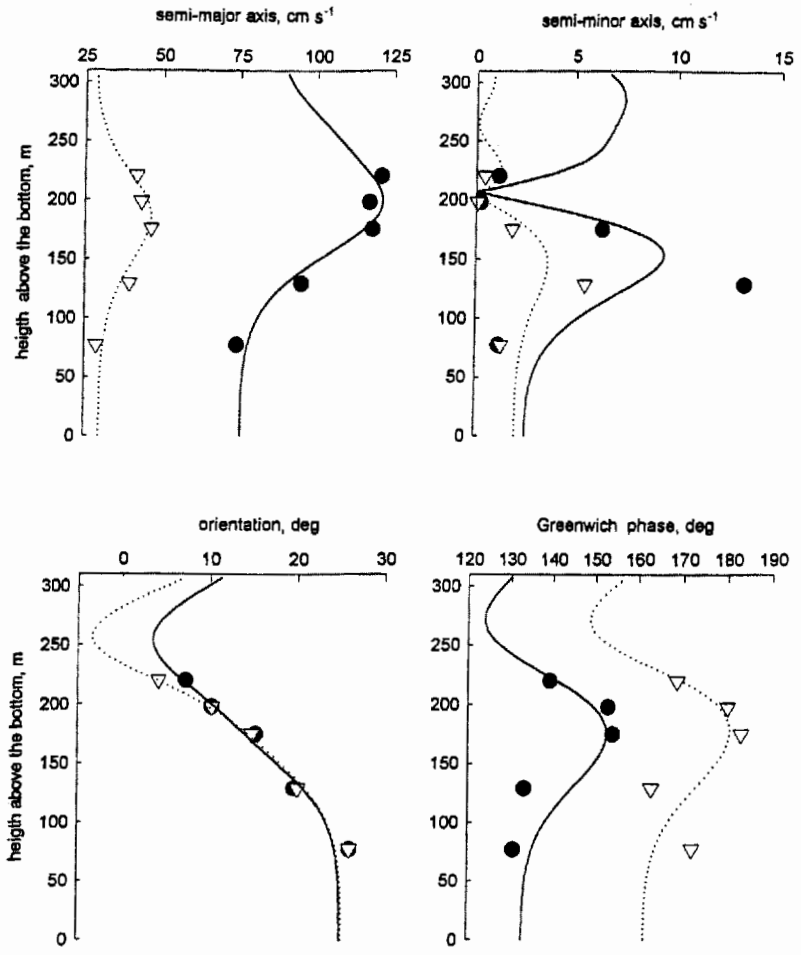


**Figure 3.** Vertical distributions of tidal current ellipse parameters for the $M_2$ (solid lines) and $S_2$ (dotted lines) waves. Solid circles and triangles indicate the observed values of the parameters.

5 shows, as suggested by the reviewer, that if there had been a shallower currentmeter at 250 m above the bottom, for example, the inference about a predominance of modes 2 and 3 over mode 1 might have been revised. That is, as the currentmeters do not span the upper part of the pycnocline, the contribution of each baroclinic mode to the observed velocity variance cannot be quantified exactly.

## 5. CONCLUSIONS

The DMD technique has been applied to the current-meter and CTD data obtained during the 1985–1986 Gibraltar Experiment and the 1989 survey to clarify some features of the $M_2$ and $S_2$ tidal currents at the Camarinal Sill. As has been established, the currents are mainly controlled by the barotropic mode and the second and third baroclinic modes with the $M_2$ and $S_2$ frequencies. Of these modes the barotropic ones are dominant. They account for 89 and 88.2 % of the observed height-averaged velocity variance at the $M_2$ and $S_2$ frequencies, respectively. The relative contributions of the second and third baroclinic modes to the current velocity variability are 5.91 and 4.24 % for $M_2$ and 4.43 and 6.18 % for $S_2$. As expected, the second and third mode velocity variances vary in magnitude at different heights according to the mode

structure and are thus conducive to changes in the vertical structure of the $M_2$ and $S_2$ tidal currents.

In particular, it is the second and third baroclinic modes that are responsible for the existence of a maximum in the vertical distribution of the semi-major axes of the $M_2$ and $S_2$ tidal current ellipses at the height of about 200 m. Also, the third baroclinic mode, along with the first one, causes the $M_2$ and $S_2$ tidal currents to reverse their sense of rotation, while the second baroclinic mode, along with the first one, produces an appreciable veering of the semi-major axes of the $M_2$ and $S_2$ tidal current ellipses in the lower 200-m layer. One more well-defined feature in the vertical distribution of tidal current ellipse parameters is a maximum of the Greenwich phase at the height of about 170 m which is associated with the third baroclinic mode.

It is worth noting that the above estimates of the relative contributions of modes 2 and 3 to the observed velocity variance as well as the inference about a predominance of these modes over mode 1 should be regarded as provisional. This is because in the case of coarse vertical currentmeter distribution the DMD technique may misrepresent the true relative contribution of each lower-order baroclinic mode.

As has been shown, the same three baroclinic modes explain, as a minimum, 90 % of the observed density amplitude variability at semidiurnal frequencies. More precisely, if at heights from 150 to 200 m the variability is predominantly due to the second mode (its fraction is about 80 %), then at heights from 230 to 280 m over 50 % of the variability is accounted for by the first mode. The relative third-mode density amplitude variance does not exceed 20 % everywhere

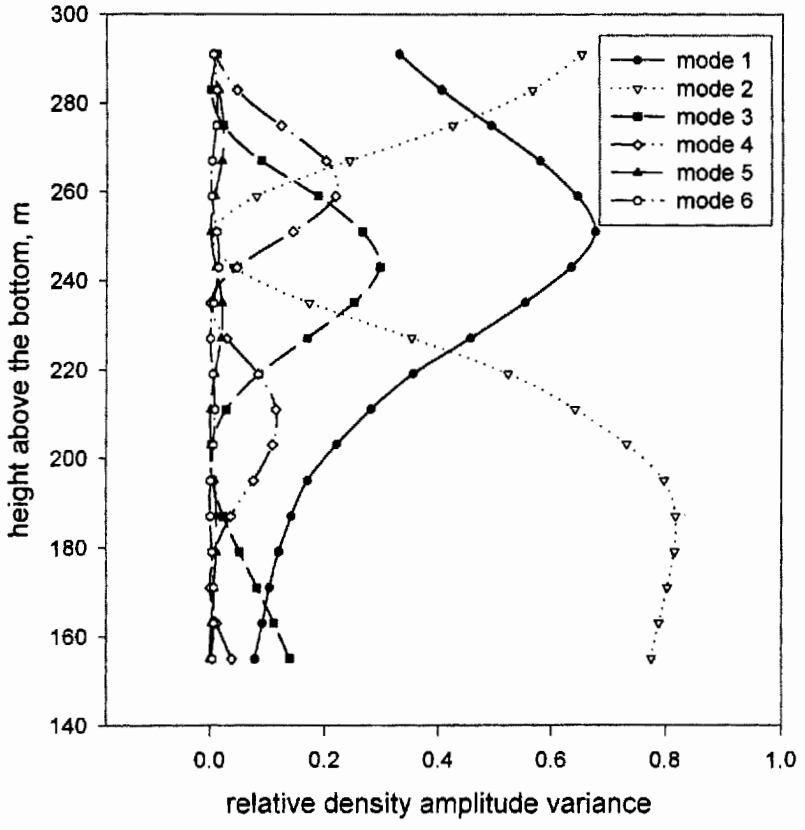


**Figure 4.** Relative mode *n* density amplitude variance as a function of height.

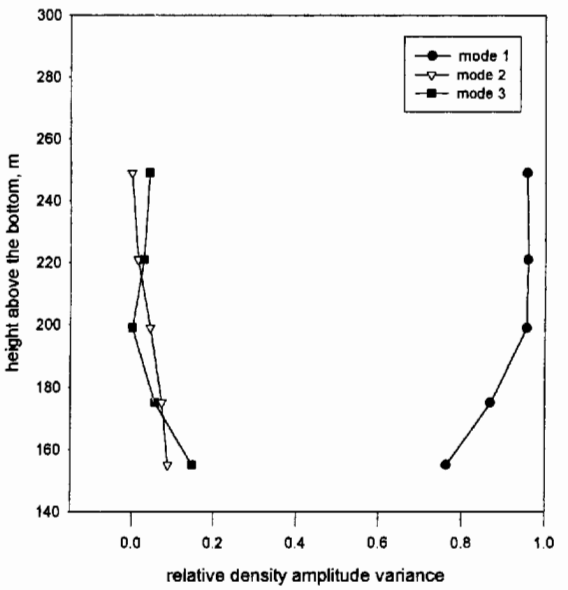


**Figure 5.** The same as in *figure 4*, but using the density time series at the currentmeter heights.

except for heights from 230 to 250 m. Here it may be as much as 35 %. The relative contribution of the higher-order modes to the density amplitude variability is assessed at about 1 % or less.

It is of interest to compare the derived estimates of the barotropic tidal current characteristics with those obtained by employing the EOF decomposition technique. Based on the DMD technique, the semi-major axis, its orientation, the Greenwich phase and the semi-minor axis of the $M_2$ tidal current ellipse are, respectively, 85.18 cm $s^{-1}$, 16.94°, 143.72° and 0.6 cm $s^{-1}$. The height-averaged values of the same ellipse parameters for the first EOF referred to as a barotropic mode are 101 cm $s^{-1}$, 16°, 148° and 4 cm $s^{-1}$. Agreement between the estimates of the orientation of the semi-major axis, the Greenwich phase and the sense of rotation (the latter is indicated by the sign of the semi-minor axis) is reasonable. The same cannot be said of the other ellipse parameters, most notably the semi-major axis, for which values in both cases differ by about 15 cm $s^{-1}$. There is a certain disparity between the values of the relative barotropic-mode velocity variance at the $M_2$ frequency. This variance is 88.8 % when employing the DMD technique and 96.55 % (92.3 or 92.7 % at semidiurnal frequencies, after [2]) when employing the EOF decomposition technique. Which of these estimates is correct? And, in general, how much are the estimates of all the other characteristics of the barotropic and baroclinic tidal currents presented here and elsewhere adequate? Also, what is the spatial distribution of the lower-order baroclinic modes in the region of interest and how is it modified by the physical configuration of the Strait of Gibraltar? The answers to these questions will remain open until new current-meter data with a fine vertical resolution becomes available.

## Acknowledgements

This work was supported by INTAS Project, no. 96-1875, the EC Project SELF II, contract number CT 95-0087, and was carried out during a stay of B.A. Kagan as visiting professor at the University of Cádiz. The authors thank the Army Hydrographic Institute of Cádiz for providing the CTD data used in this work and the reviewers for helpful comments on the manuscript.

## REFERENCES

[1] Bray N.A., Winant C.D., Kinder T.H., Candela J., Generation and kinematics of the internal tide in the Strait of Gibraltar, in: Pratt L.J. (Ed.), The Physical Oceanography of Sea Straits, Kluwer Academic Publishers, Dordrecht, 1990, pp. 477–491.

[2] Candela J., Winant C.D., Ruiz A., Tides in the Strait of Gibraltar, J. Geophys. Res. 95 (1990) 7317–7335.

[3] Kundu P.K., Allen J.S., Smith R.L., Modal descomposition of the velocity field near the Oregon coast, J. Phys. Oceanogr. 5 (1975) 638–704.

[4] Mañanes R., Bruno M., Alonso J., Fraguela B., Tejedor L., The nonlinear interaction between tidal and subinertial flows in the Strait of Gibraltar, Oceanol. Acta 21 (1998) 33–46.

[5] Marchuk G.I., Kagan B.A., Internal gravitational waves in a really stratified ocean, Izvestiya Akad Nauk SSSR, Atm. Ocean. Phys. 6 (1970) 412–422.

[6] Müller T.J., Siedler G., Multi-year current time series in the eastern North Atlantic Ocean, J. Mar. Res. 50 (1992) 63–98.

[7] Schott F., On the energetics of baroclinic tides in the North Atlantic, Ann. Geophys. 33 (1977) 41–62.

[8] Siedler G., Paul U., Barotropic and baroclinic tidal currents in the eastern basins of the North Atlantic, J. Geophys. Res. 96 (1991) 22259–22271.

[9] Tejedor L., Izquierdo A., Kagan B.A., Sein D.V., Simulation of the semidiurnal tides in the Strait of Gibraltar, J. Geophys. Res. 104 (1999) 13541–13557.